Theoretical study for regulatory property of scaffold protein on MAPK cascade: A qualitative modeling

Ming Yi, Kelin Xia, Meng Zhan *

Wuhan Institute of Physics and Mathematics, Chinese Academy of Sciences, Wuhan 430071, China

ABSTRACT

An integrated mathematical model, which incorporates scaffold proteins into a mitogen-activated protein kinases cascade, is constructed. By employing Monte Carlo simulation, regulatory property of scaffold protein on signaling ability for the mitogen-activated protein kinases cascade is investigated theoretically. It is found that (i) scaffold binding increases signal amplification if dephosphorylation is slow and decreases amplification if dephosphorylation is rapid. Also, increasing the number of scaffold decreases amplification if dephosphorylation is slow. (ii) The scaffold number can control the timing of kinase activation so that the time flexibility of signaling is enhanced. (iii) It is observed that for slow dephosphorylation case, scaffolds decrease the sharpness of the dose–response curves. While for fast dephosphorylation case, increasing scaffold number decreases the height of response, but the shape of graded response is sustained. Furthermore, the underlying mechanism and the correlation of our results with real biological systems are clarified.

Crown Copyright © 2010 Published by Elsevier B.V. All rights reserved.

1. Introduction

By a typical motif in signal transduction network, i.e., mitogen-activated protein kinases (MAPK) cascade [1,2], specific signals from cellular membrane are converted into the specific gene expression pattern in nuclear and finally appropriate cell fate. A MAPK cascade consists of three sequentially acting kinases, including MAPKKK (A), MAPKK (B) and MAPK (C), which are located in three different layers as shown in Fig. 1. Each kinase, if activated, can activate its downstream substrate by phosphorylation reaction. The activated kinases can be deactivated by phosphatases by a dephosphorylation reaction. For simplicity, a generic phosphatases (P) is considered here. It is clear three enzyme cycles i.e., six enzymatic reactions are involved in the biochemical network.

The MAPK signaling cascade is perhaps one of the most well studied signal cascades, both experimentally and computationally [3–8]. This central cascade is critical for governing cell growth and proliferation as well as actin cytoskeleton rearrangement [9]. Therefore, signaling cascades become a very vibrant topic in several different avenues of research recently. A signaling cascade in calcium signaling is constructed by mathematical modeling [10,11], it is found that a two-level protein cascade can act as a band-pass filter for time-limited oscillations. The band-pass filters are then combined into a

network of MAPK signaling cascades that by filtering the frequency of time-limited oscillations selectively switches cellular processes on and off. The wide applicability and robustness of MAPK cascade are also given in general [12]. Studies have observed that magnitude and duration of MAPK activation encodes specificity, the crosstalk of cAMP pathway with MAPK related to the phenotypic response in contributing towards specificity are clarified [13,14]. In addition, the role of MAPK cascade for oncogene detection and FLO11 expression is also investigated [15].

There exists a kind of macromolecule, i.e., scaffold proteins in different signal pathway, such as MAPK pathway, calcium signaling, innate immune signaling scaffolds [16–20]. Each scaffold proteins can bind three kinases and form a complex, which often plays important roles on accurate biological response. In such pathways, they regulate signal transduction and help localize pathway components (organized in complexes) to specific areas of the cell such as the plasma membrane, the cytoplasm, the nucleus, the golgi, endosomes, and the mitochondria. Scaffold proteins act in at least four ways: tethering signaling components, localizing these components to specific areas of the cell, regulating signal transduction by coordinating positive and negative feedback signals, and insulating correct signaling proteins from competing proteins.

The signaling feature of signal transduction in the presence of scaffold protein is an important subject theoretically where there is much that is not understood. A quantitative computer model of MAPK cascade with a generic scaffold protein is provided by A. Levchenko et al. [18]. Analysis of this deterministic model reveals that formation of scaffold–kinase complexes can be used effectively to regulate the

* Corresponding author.
E-mail addresses: yiming@wipm.ac.cn (M. Yi), zhanmeng@wipm.ac.cn (M. Zhan).
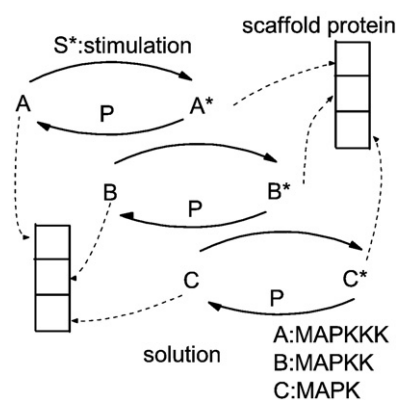
Fig. 1. A simple description for the biochemical process of MAPK cascade. The scaffold protein can bind three kinases orderly. It is noted that signal input S^*, which is activated nearby the cell membrane, can move into the cytoplasm and activate A both in solution and on scaffold.

Fig. 2. Schematics are shown for the simulation of signaling events related with scaffold protein. (a) The scaffold and its specific three binding sites. (b)–(c) The binding or unbinding events with probabilities P_B or P_{UB}. (d) The activation reactions occur on the scaffold by one-step mechanism with probabilities G. (e) The activation and deactivation reactions between the molecules in the solution and on the scaffold is also assumed by one-step mechanism.

specificity, efficiency, and amplitude of signal propagation. The effect of scaffold protein on dose–response (i.e., input–output character-istics) of a signaling system has been studied theoretically [18,21,22], it has been suggested that scaffolds can affect the dose–response curves.

Most of previous researches are based on the deterministic ordinary differential equation model, however for the cell conditions, two important factors must be considered. (i) The number of protein molecules are often low, so the biochemical reactions are random, occurring with certain reaction probabilities. The stochasticity, which is often called as internal noise, is resulted from the small cell size and cannot be omitted. The effects of internal noise in the level of single cell on variable biological behaviors, such as spatial periodicity in excitable media, intracellular and intercellular calcium wave propa-gation, are studied extensively [23–29]. (ii) In addition, the spatial effect is also an important factor under small cell size [30–32]. The enzyme and substrate molecules diffuse in the reaction space with finite velocity. Spatial diffusion leads to that the biochemical system cannot be treated with a well-stirred system. As our knowledge, the combined effects of stochastic noise and spatial diffusion are still studied in few researches about the signaling pathway. Therefore, in this article, we propose a mathematical model in which scaffold protein is integrated into the MAPK cascade. We use a stochastic reaction diffusion scheme to investigate the role of the scaffold protein therein by Monte Carlo simulation. Following the description of the model, the impacts of the scaffold protein on the signaling ability of the MAPK for both slow and fast dephosphorylation cases are investigated numerically. It is shown that, within the newly proposed model, scaffold proteins can regulate different cellular functions and that the number of scaffold proteins can control the timing of kinase activation. In addition, some interesting results for dose–response curves are also clarified.

2. Modeling and simulation

An initial signaling stimulus is S^*, which represents small G-protein (e.g., *Ras-GTP*) that has already been activated by membrane proximal events. We do not consider how the signaling input is activated nearby the membrane, the input in our simulation for MAPK cascade is just the activated signaling S^*. After signaling input S^* moves into the cytoplasm, it can activate A both in the solution and on the scaffold. In order to investigate the roles of scaffold protein on MAPK cascade, a biological model which incorporates the scaffold protein into MAPK cascade is built. The combined model is shown in Fig. 1, furthermore, the interactions between the protein in the solution and that on the scaffold are summarized in Fig. 2.
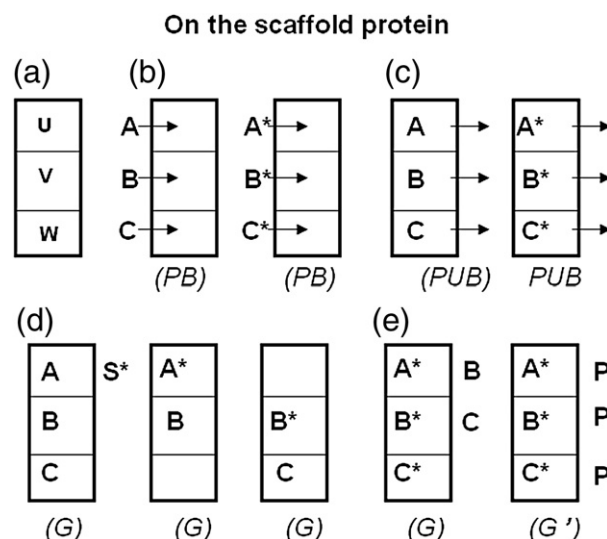
Each scaffold protein contains three specific binding sites provided for three different kinases, therefore it occupies three lattice sites. We allow both inactive and active kinases to potentially bind to their specified binding sites.

Active A^* on the scaffold can active B both on the scaffold and in the solution, active B^* on the scaffold can active C both on the scaffold and in the solution. However, the active A^* in the solution can active B in the solution but not B on the scaffold. The active B^* in the solution can active C in the solution but not C on the scaffold. Of course, the real interaction between the kinase protein in the solution and that on the scaffold is not clear, so some rules can be adjusted, e.g., we can allow active A^* in the solution to active B both in the solution and on the scaffold, but the consideration is beyond our aim in this article.

Each kinase activation (i.e, phosphorylation) or deactivation (i.e., dephosphorylation) reaction in the solution is treated by a two-step enzymatic mechanism as below: firstly, the kinase (or phosphatase) and its substrate associate into an intermediate bimolecule complex by a reversible reaction, then the complex disassociate into the active or inactive products by a catalysis reaction. For simplicity, the kinase activation or deactivation on the scaffold is treated by a single-step collision mechanism.

Our Monte Carlo (MC) simulation is performed on 2 dimension square lattices 100×100 with reflecting boundary conditions. Each protein molecule (unimolecule or bimolecule) only can occupy one lattice site. Except for scaffold protein, each molecule type is mobile on the lattice through diffusion. The diffusion event is modeled by independent (nearest-neighbor) random walk of the individual molecules. The probability of diffusion is denoted with P_D. At the beginning of simulation, the S^*, A, B, C and P molecules are placed on the lattice by randomly choosing the coordinates for each of them. At each MC step, all occupied lattice sites are chosen at random with uniform probability.

In our simulation, when two appropriate proteins come into contact with each other by diffusion, certain a biochemical reaction may occur. Each stochastic reaction event has one corresponding reaction probability. In solution, for activation process of kinase A, B and C, three probabilities are marked (see reactions (1)–(3)): the probability of association reaction F, the probability of disassociation reaction R, and the probability of catalysis reaction G. For deactivation

process of A^*, B^* and C^*, three corresponding probabilities, i.e., F', R' and G', are also required (see reactions (4)–(6)).

$$S^* + A \underset{R}{\overset{F}{\rightleftharpoons}} S^*A \overset{G}{\rightarrow} S^* + A^*, \tag{1}$$

$$A^* + B \underset{R}{\overset{F}{\rightleftharpoons}} A^*B \overset{G}{\rightarrow} A^* + B^*, \tag{2}$$

$$B^* + C \underset{R}{\overset{F}{\rightleftharpoons}} B^*C \overset{G}{\rightarrow} B^* + C^*, \tag{3}$$

$$A^* + P \underset{R'}{\overset{F'}{\rightleftharpoons}} A^*P \overset{G'}{\rightarrow} A + P, \tag{4}$$

$$B^* + P \underset{R'}{\overset{F'}{\rightleftharpoons}} B^*P \overset{G'}{\rightarrow} B + P, \tag{5}$$

$$C^* + P \underset{R'}{\overset{F'}{\rightleftharpoons}} C^*P \overset{G'}{\rightarrow} C + P. \tag{6}$$

The scaffold protein should be a mobile molecule. However, because it also is a macromolecule, the diffusion rate is much smaller than that of small kinase proteins in the solution so that our simulation is time-consuming if the diffusion of scaffold is considered. For simplicity, we regard the scaffold as an immobile and rigid molecule at present. In addition, the interaction between the kinase in the solution and on the scaffold is very complex, the simulation scheme becomes very difficult if we consider it as a mobile molecule. Therefore, in our article, we only focus our attention on the effect of scaffold binding and scaffold number, and neglect the diffusion of scaffold.

Each scaffold protein has three specific binding sites (U, V and W) provided for three different kinases (A, B and C) (see Figs. 1 and 2(a)). As shown in Fig. 2(b)–(c), the binding (or unbinding) of inactive and active kinases to (or from) their specified binding sites is allowed with probability of P_B (or P_{UB}). In order to bind to or unbind from the scaffold, we assume the kinase protein should overcome a thermal energy barrier E_B or E_{UB}. The consideration is qualitatively similar in many cases for catalytic mechanisms. The probability of binding (or unbinding) is computed directly from the energy barrier of binding E_B (or unbinding E_{UB}), i.e., $P_B = e^{-E_B}$ (or $P_{UB} = e^{-E_{UB}}$). It is noted that these probabilities are almost certainly not quantitatively accurate, however for our qualitative theoretic study, it is still valid to some extent.

In the article, for each scaffold protein, three specific binding sites, provided for three protein kinases A (and A^*), B (and B^*), C (and C^*), are denoted with U, V and W, respectively (see Fig. 4(a)). We denoted the A, B and C on their corresponding binding site with AU, BV and CW. We denoted the A^*, B^* and C^* on their corresponding binding site with A^*U, B^*V and C^*W.

The system we simulated consists of 200 A, 200 B, 1000 C, 200 S^* and 600 generic P species. The total number of protein is 2200. All through our article, $E_B = 0.0$, i.e., $P_B = 1.0$. The larger the E_{UB} is, the smaller the P_{UB}, hence the kinases bind to scaffold protein more tightly. The probability of diffusion $P_D = \frac{1}{2 \times 2} D^{eff}$, where D^{eff} denotes the diffusion time scale, $D^{eff} = 0.1$ [20]. The diffusion constant used in our simulations is 1(lattice spacings)^2/MCstep, and taking a value of the lattice spacing to be 10 nm (nearly the diameter of one protein). It is derived that one MC step corresponds to about 1 μs in real signaling system. In our simulation, the signaling time is just recorded with the number of MC step. Initially, all the scaffold proteins are placed as separately as possible. That is to say, no two scaffold proteins are close to each other. If allowing two scaffolds to be neighbor, different simulation trial may cause different distribution of scaffold and mainly lead to different neighbor number of scaffold, the simulation results would change greatly with different trials. While our consideration not

allowing any two scaffold to be neighbor can reduce the difference of different simulation trial. In this study, for activation process (1)–(3), three reaction probabilities are $F = 1$, $R = 0.02$ and $G = 0.04$, which are assumed in [33]. For deactivation process (4)–(6), F', R' and G' are given empirically dependent on slow or fast dephosphorylation case investigated below.

After a dynamic steady-state is reached, the signaling ability of cascade is studied. For simplicity, A^*, B^* and C^* are used to represent the number of three active kinases, respectively. To measure the signaling ability, signaling amplification $\phi = C^*/A^* - 1$ is used. The mean signaling amplification is given through $\phi_0 = <\phi>$, $<>$ denotes the average of long enough time at the steady state. Next, we focus our attention on the roles of (i) the scaffold binding (measured by E_{UB}) and (ii) the number of scaffold protein (controlled by NS) on signaling amplification of MAPK cascade.

3. Results

3.1. Roles of scaffold binding on signaling ability

In this subsection, the roles of scaffold binding on signaling ability are investigated. The scaffold number $NS = 200$, is fixed. As a control parameter, E_{UB} is changed from 0.0 to 20.0. When E_{UB} increases, it implies the kinase can more easily bind to the scaffold. For simplicity, only three E_{UB} are used. The unbinding probability covers a wide enough range from $P_{UB} = e^{-0.0} = 1.0$ to $P_{UB} = e^{-20.0}$. Below, slow and fast dephosphorylation cases are explored respectively.

In order to provide a slow dephosphorylation case, three reaction probabilities in deactivation process (4)–(6) are given as $F' = 0.0001$, $R' = 0.00002$ and $G' = 0.00004$. Here the selection is arbitrary, however the qualitative results provided below are still genetic for understanding the mechanism of real signaling cascade. The evolutions of number of active kinases A^*, B^* and C^* (shown in the left column in Fig. 3) and signaling amplification (shown in the right column in Fig. 3) for three different E_{UB} are given respectively. (i) When E_{UB} is small (Fig. 3(a)) or moderate (Fig. 3(c)), it is found three active kinases arrive at their steady states quickly. In addition, as shown in Fig. 3(b) and (d), the signaling amplification reaches a steady state with very small fluctuation. Especially, it is observed the time course for A^* (black line) coincides with that for B^* (red line). It seems that if the initial numbers are same ($A = B = 200$), then the signaling abilities of A^* and B^* are undistinguishable. (ii) When the scaffold binding is very strong, it takes three active kinases longer time to arrive their steady states (Fig. 3(e)), the corresponding signaling amplification also arrives at steady state very slowly, 500,000 MC steps is required (Fig. 3(f)). An interesting phenomena, different with the observation in Fig. 3(a) and (c), appears that there are not any coincidence between the time courses for A^* and B^* (Fig. 3(e)), which indicates that the kinase activities between them are distinguishable. For a cascade, we conclude if the initial numbers of two kinases in different layers are same, in order to judge their different signaling abilities, it is necessary to make the function of scaffold protein strong enough (about $E_{UB} \geq 10.0$).

In order to provide a fast dephosphorylation case, the basal phosphatase activity should be set to a high level, which makes the cascade intrinsically difficult to activate. Therefore, as an example, three reaction probabilities in deactivation process (4)–(6) are given as $F' = 1.0$, $R' = 0.02$ and $G' = 0.04$. The time evolutions of the total number of active kinases A^* and C^* (shown in the left column in Fig. 4) and signal amplification (shown in the right column in Fig. 4) for three different E_{UB} are plotted respectively. (i) The scaffold binding is strong enough for $E_{UB} = 20.0$. As observed in Fig. 4(a), after a long transient time, the number of active A^* fluctuates persistently with a large amplitude, while C^* disappears. Therefore, the signal amplification becomes zero at last as shown in Fig. 4(b). (ii) Decreasing the scaffold binding to $E_{UB} = 10.0$, it is found active protein kinase A^* and C^* both
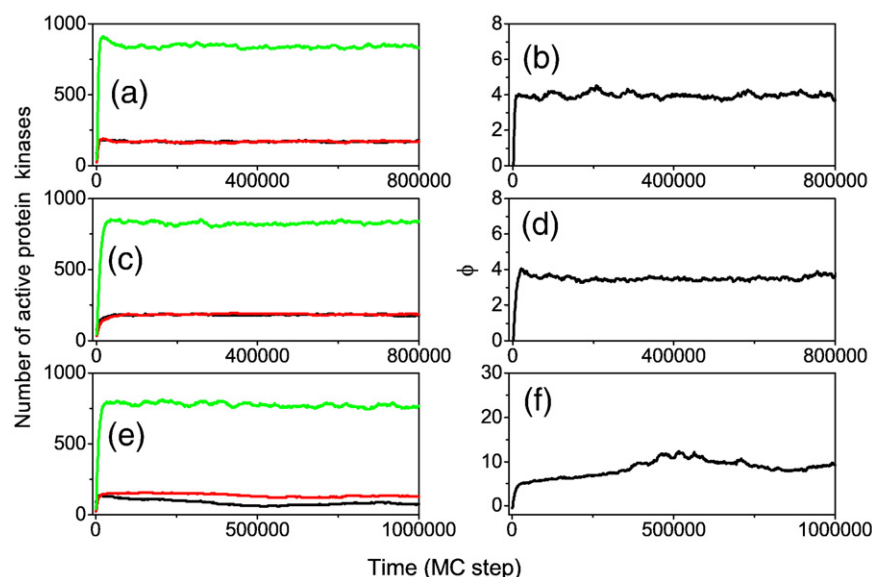
Fig. 3. For slow dephosphorylation case, time evolutions of kinases number A^* (black lines), B^* (red lines) and C^* (green lines) shown in the left column and time evolutions of signaling amplification shown in the right column for three different E_{UB}. From top to bottom: (a)–(b) $E_{UB} = 0.0$. (c)–(d) $E_{UB} = 6.0$. (e)–(f) $E_{UB} = 10.0$. (For interpretation of the references to color in this figure legend, the reader is referred to the web version of this article.)

fluctuate observed in Fig. 4(c). The signaling amplification also changed randomly with time, as shown in Fig. 4(d). In most of time, the signaling amplification is negative, so the signaling is attenuated when it passes across the MAPK cascade. Occasionally, the signaling amplification becomes positive and the signaling is amplified. It is obvious that the MAPK cascade under such a weak phosphorylation case is not a stable biological control system. (iii) Decreasing the scaffold binding furthermore, so that it is very weak for $E_{UB} = 20.0$, it is found the active protein kinase A^* and C^* fluctuate with larger amplitude, and the mean number of A^* and C^* are also enhanced as shown in Fig. 4(e). As observed in Fig. 4(f), the signaling amplification oscillates stochastically around zero.

The effects of scaffold binding on signaling ability under this slow and fast dephosphorylation case are summarized in Fig. 5(a) and (b), respectively. For slow dephosphorylation case, with increasing the scaffold binding by enhancing E_{UB}, the mean signaling amplification is nearly unchanged initially and is insensitive to the change of scaffold function. After a transition point $E_{UB} \approx 7.5$, the mean signaling amplification increases, therefore the scaffold proteins allows a more effective propagation of signal. The result indicates that the scaffold protein can play a constructive role. For fast dephosphory-lation case, with increasing E_{UB}, the mean signaling amplification decreases monotonously. Our simulation results suggest that, due to the modulation of scaffold binding, kinase cascades can operate in
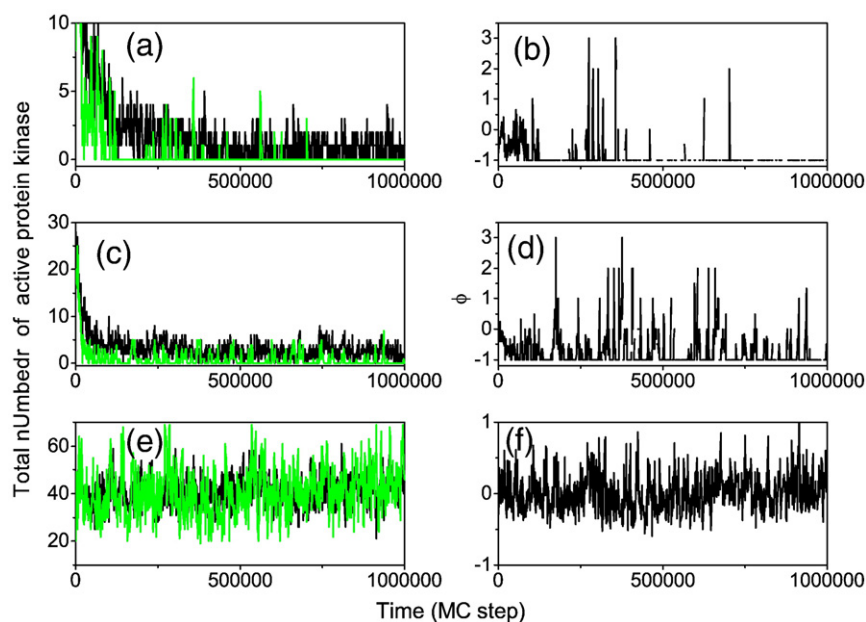

Fig. 4. For fast dephosphorylation case, time evolutions of A^* (black lines) and C^* (green lines) shown in the left column and time evolutions of signaling amplification shown in the right column for three different E_{UB}. From top to bottom: (a)–(b) $E_{UB} = 20.0$. (c)–(d) $E_{UB} = 10.0$. (e)–(f) $E_{UB} = 0.0$. (For interpretation of the references to color in this figure legend, the reader is referred to the web version of this article.)
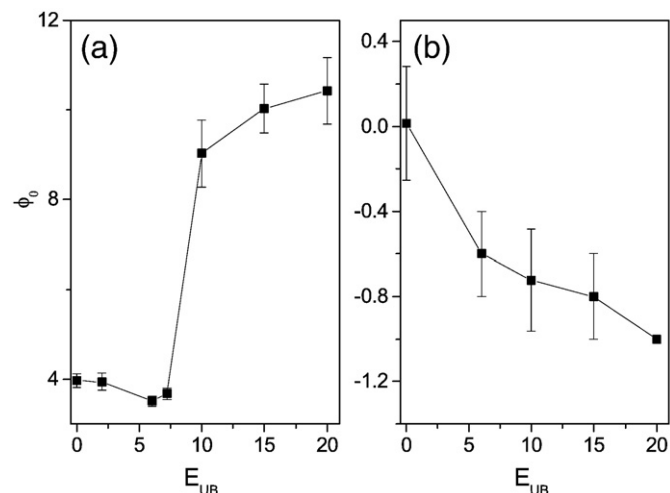
Fig. 5. Dependence of mean signaling amplification on the scaffold binding for a fixed scaffold number $NS = 200$. (a) Slow dephosphorylation case. (b) Fast dephosphorylation case.

different dynamical regimes under different physiological conditions so that signaling ability is enhanced, attenuated, or even invariable.

Though the results above are very difficult to illustrate by some simple mechanisms at present, we still give some qualitative interpretations by two different ways.

Firstly, our views about the control mechanism of scaffold protein are set forth through the detailed dynamics of different components of kinase. As shown below, as an example, the time evolutions of different forms of kinases under slow dephosphorylation case (i.e. Fig. 5(a)) when adjusting E_{UB} are explored. Three forms of protein kinases are chosen: the first one is the inactive form of three kinases bond at their corresponding site on the scaffold, i.e., AU, BV and CW. The second one is the active form of three kinases on the scaffold i.e., A^*U, B^*V and C^*W. The third one is the active form of three kinases in the solution, i.e., A^*S, B^*S and C^*S. For convenience, the number of each form is denoted with their corresponding kinase name. (i) As show in Fig. 6(a)–(c), $E_{UB} = 0.0$, the scaffold binding is very weak due to the large P_{UB}. Therefore, the active (red lines) and inactive (black lines) kinases on the scaffold protein both are few, such relations are provided by three coarse equations $AU + A^*U \approx 7$ (Fig. 6(a)), $BV + B^*V \approx 7$ (Fig. 6(b)) and $CW + C^*W \approx 0$ (Fig. 6(c)). And nearly all active kinases exist in the solution (green lines). (ii) As show in Fig. 6(d)–(f), $E_{UB} = 6.0$, the scaffold binding becomes strong. Now all the scaffolds are almost occupied by the inactive and active kinase A and B, e.g., $AU + A^*U \approx 200$ (Fig. 6(d)) and $BU + B^*U \approx 200$ (Fig. 6(e)). While it is strange to found that few C are bound to the scaffold proteins under such large scaffold binding (shown in Fig. 6(f), i.e., $CU + C^*U \approx 0$. In addition, most (75%) of active protein A^*U (see red line in Fig. 6(d)) and B^*V (see red line in Fig. 6(e)) exist on the scaffold. Active protein kinases exist in the solution are smaller than that on the scaffold. (iii) As show in Fig. 6(g)–(i), $E_{UB} = 10.0$, the scaffold binding is strong enough. It is found that the active kinase in the solution are reduced remarkably. We also find the active and inactive kinase
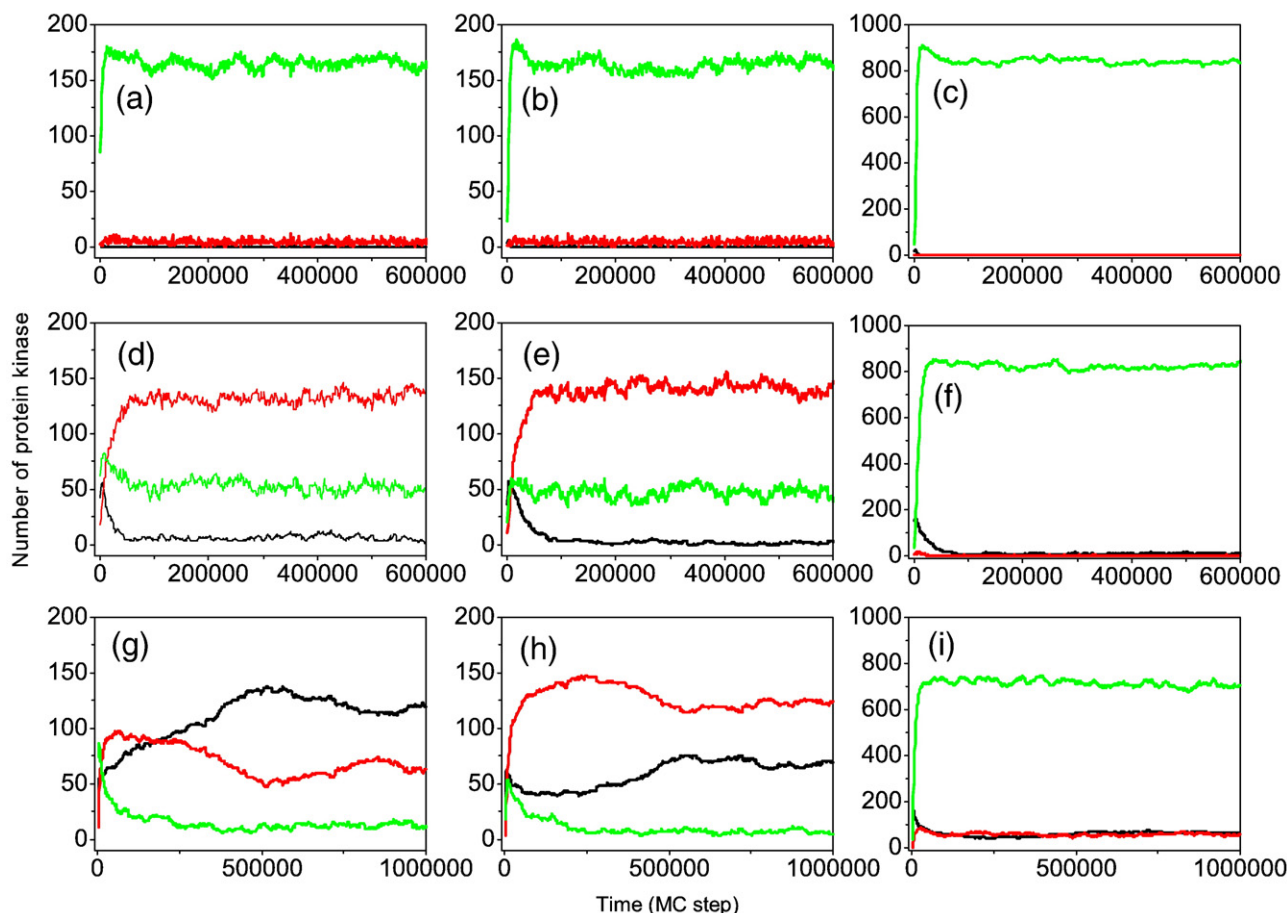

Fig. 6. Time evolutions of kinases number for three different E_{UB} under slow dephosphorylation case. From top to bottom: (a)–(c) $E_{UB} = 0.0$. (d)–(f) $E_{UB} = 6.0$. (g)–(i) $E_{UB} = 10.0$. The left column: the evolution of AU, A^*U and A^*S. The middle column: the evolution of BV, B^*V and B^*S. The right column: the evolution of CW, C^*W and C^*S. AU, BV and CW are shown with black lines, A^*U, B^*V and C^*W are shown with red lines, A^*S, B^*S and C^*S are shown with green lines. (For interpretation of the references to color in this figure legend, the reader is referred to the web version of this article.)
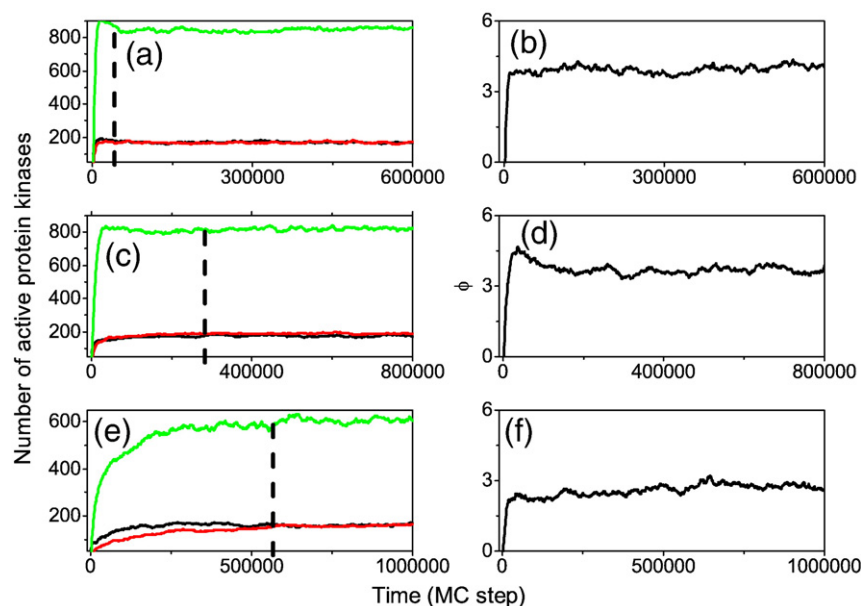
Fig. 7. For slow dephosphorylation case, time evolutions of A^* (black solid lines), B^* (red solid lines) and C^* (green solid lines) shown in the left column and time evolutions of signaling amplification shown in the right column for three different *NS*. From top to bottom: (a)–(b) *NS* = 2. (c)–(d) *NS* = 200. (e)–(f) *NS* = 600. (For interpretation of the references to color in this figure legend, the reader is referred to the web version of this article.)

protein *C* can now occupy some scaffold sites, e.g., $CU + C^*U \approx 100$. In a word, the result shows qualitatively that the increase of the scaffold binding facilitates the signaling, the increase of signaling amplification mainly comes from the decreasing of active kinase C^* in solution.

Secondly, the different regulatory property of scaffold under different conditions can be illustrated by a competition mechanism between the constructive and the destructive roles played by scaffold. Under slow dephosphorylation case, the destructive role of scaffold is caused by a stoichiometric constraint, i.e., scaffold limits the number of molecules of the inactive downstream target that can potentially be

phosphorylated. While the constructive role of scaffold is resulted from that the spatial proximity of kinases on a scaffold reduces the encounter time so that the inactive proteins downstream can be activated more easily. In order to determine the regulatory property of scaffold, we only need to judge which role dominates over the other role of scaffold. As shown in Fig. 5(a), when the scaffold binding is increased with enhancing E_{UB}, the encounter time of inactive protein with scaffold is decreased, therefore the constructive role becomes stronger. At the same time, the scaffold number is not large for *NS* = 200, the scaffold only can limit small number of inactive
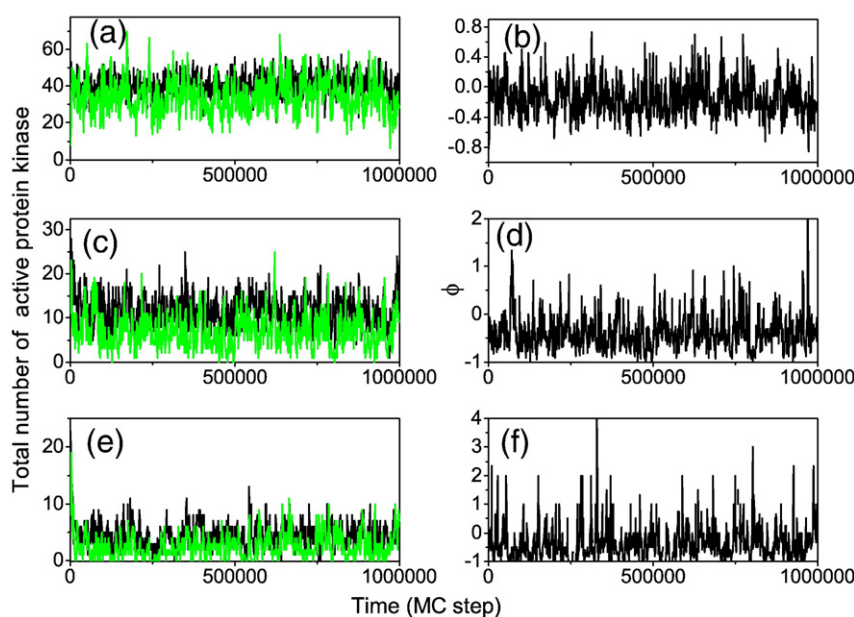

Fig. 8. For fast dephosphorylation case, time evolutions of A^* (black lines) and C^* (green lines) shown in the left column and time evolutions of signaling amplification shown in the right column for three different *NS*. From top to bottom: (a)–(b) *NS* = 2. (c)–(d) *NS* = 200. (e)–(f) *NS* = 600. (For interpretation of the references to color in this figure legend, the reader is referred to the web version of this article.)
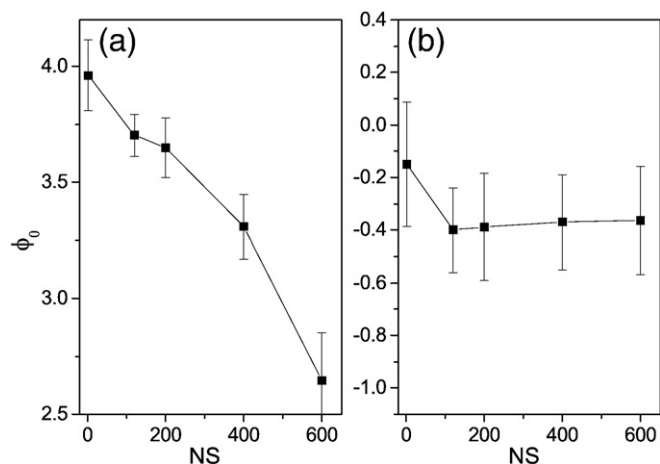
Fig. 9. Dependence of mean signaling amplification on the scaffold number for a fixed scaffold binding $E_{UB} = 7.2$. (a) Slow dephosphorylation case. (b) Fast dephosphorylation case.

downstream target, hence the destructive role is weak. The constructive role of scaffold protein dominates the cascade so that scaffold binding facilitates the signaling amplification.

3.2. Roles of scaffold number on signaling ability

In this subsection, the effects of scaffold number on signaling ability are investigated. Energy of unbinding from the scaffold is taken to be $E_{UB} = 12\ k_B T \approx 7.2$ kcal/mol, which is typical [34] ($k_B T$: Boltzman's thermal energy). As a control parameter, the number of scaffold protein is changed from to 2 to 600.

For slow dephosphorylation case, the time evolutions of active kinases number A^*, B^* and C^* (shown in the left column in Fig. 7) and signaling amplification (shown in the right column in Fig. 7) for three different *NS* are plotted. (i) It is clear the three signaling cascades all achieve steady states with small fluctuation. (ii) E_{UB} used here is not strong enough to make an identification between the time courses for A^* (black solid line) and B^* (red solid line), therefore the signaling dynamics of them are similar for any *NS* after transient state, as shown in Fig. 7(a), (c) and (e). (iii) Furthermore, it is found that larger *NS* is, larger the time required to reach their steady states (see dashed lines shown in Fig. 7(a), (c) and (e)). The results indicate that number of scaffold protein can control the timing of kinase activation, leading to signal at a wide time region. Thus, the time flexibility of signal is enhanced. (iv) As exhibited in Fig. 7(b), (d) and (f), the signaling amplification is positive, so the signal is always amplified stably as it propagates along the cascade.
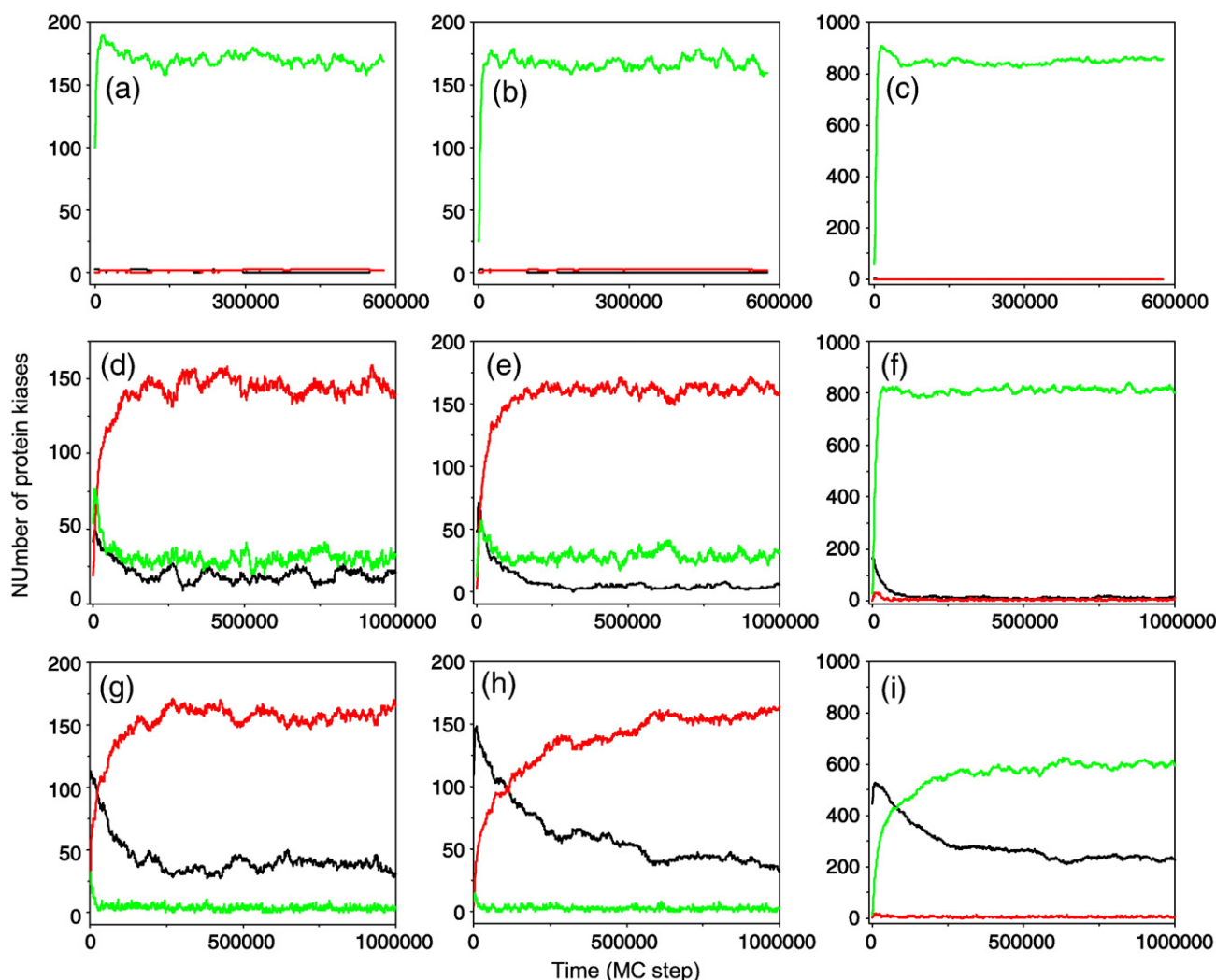

Fig. 10. Time evolutions of kinases number for three different *NS* under slow dephosphorylation. (a)–(c) *NS* = 2. (d)–(f) *NS* = 200. (g)–(i) *NS* = 600. The left column: the evolution of *AU*, A^*U and A^*S. The middle column: the evolution of *BV*, B^*V and B^*S. The right column: the evolution of *CW*, C^*W and C^*S. *AU*, *BV* and *CW* are shown with black lines, A^*U, B^*V and C^*W are shown with red lines, A^*S, B^*S and C^*S are shown with green lines. (For interpretation of the references to color in this figure legend, the reader is referred to the web version of this article.)

For fast dephosphorylation case, the time evolutions of total number of activate protein kinase A^* and C^* (shown in the left column in Fig. 8) and signal amplification (shown in the right column in Fig. 8) for three different NS, are plotted respectively. It is obvious that A^* and C^* both fluctuate around their steady states with large amplitude. With increasing the number of scaffold, the mean number of A^* and C^* decrease. The signaling amplification oscillates around zero with large noise.

The effects of scaffold number for slow and fast dephosphorylation cases are summarized in Fig. 9. For slow dephosphorylation case (Fig. 9(a)), with increasing NS, the mean signaling amplification is decreased monotonously, which exhibits a destructive role of scaffold protein. For fast phosphorylation case (Fig. 9(b)), with increasing NS, the signaling amplification is decreased firstly then reaches a plateau region. Globally, the signaling ability has very slight dependence on the scaffold number. For both cases, no constructive role of scaffold is shown.

We also give some qualitative explanation about the results under slow dephosphorylation case (i.e. Fig. 9(a)) by two ways.

Firstly, the dynamic of protein kinases in the solution and on the scaffold are investigated in detail. Similar to Fig. 6, three forms of protein kinases are shown in Fig. 10. (i) It is found most of kinases A and B exist on the scaffold protein. For example 80% of A and B when $NS = 200$ (Fig. 10(d) and (e)) and 90% of A and B when $NS = 600$ (Fig. 10(g) and (h)) are bond on the scaffold. Most of kinase A and B on the scaffold are activated. For example $\frac{A^*U}{A^*U + AU} \approx 0.95$ when $NS = 200$ (Fig. 10(d)) and $\frac{A^*U}{A^*U + AU} \approx 0.80$ when $NS = 600$ (Fig. 10(g)). Overall, for the scaffold binding given here, the dynamics of three forms for kinase A and B are nearly same, and kinase A and B both have strong interaction with the scaffold protein. (ii) However, the dynamic of kinase C is different. For $NS = 2$ and $NS = 200$, there is nearly no kinase C on the scaffold, and also few active kinases C^* are on the scaffold (see red lines in Fig. 10(c) and (f)), which is strange for this strong scaffold binding. Only when $NS = 600$, a part of kinases C begin to bind to the scaffold protein (black line in Fig. 10(i)). But the C^*W is still few (red line in Fig. 10(i)). Our results show, even if the scaffold binding is strong, that kinase C has weak interaction with the scaffold protein unless NS is large enough. (iii) For $NS = 2$ and $NS = 200$, the total numbers of active kinase on the steady states are

nearly same for A, B and C (compared Fig. 10(a) with Fig. 10(c)). However the dynamics for three forms of each kinase is very different. For $NS = 2$ as show in Fig. 10(a)–(c), due to the very small number of scaffold protein, all active kinase exist in the solution. On the contrary, for $NS = 200$ observed in Fig. 10(d)–(f), most of activate A^* and B^* exist on the scaffold, the number of activate form in the solution is small. In sum, the result shows qualitatively that the increase of scaffold number inhibits the signaling amplification.

Secondly, the different regulatory property of scaffold under different conditions can be illustrated by the competition mechanism between the constructive and the destructive roles played by scaffold. As shown in Fig. 9(a), when increasing the scaffold number, the scaffold can limit larger number of inactive downstream target, therefore the destructive role is stronger. At the same time, the scaffold binding is not strong enough for $E_{UB} = 7.2$, the encounter time of inactive protein with scaffold is not reduced largely, therefore the constructive role is not obvious. The destructive role of scaffold protein controls the cascade so that scaffold binding inhibits the signaling amplification.

4. Discussions

In conclusion, an integrated model, in which scaffold proteins are combined into a MAPK cascade, is constructed by a stochastic reaction diffusion scheme. Our modeling and simulation are not based on real reaction and diffusion rate constants but nine probabilities which are given qualitatively. Based on the qualitative mathematical model and MC simulation, we mainly investigate the regulatory roles of scaffold binding (E_{UB}) and number of scaffold protein (NS) on signaling amplification. Rich regulatory properties are exhibited by our MC simulation. Firstly, scaffold binding increases signal amplification if dephosphorylation is slow and decreases amplification if dephosphorylation is rapid. Also, increasing the number of scaffolds decreases amplification if dephosphorylation is slow. Secondly, for a cascade, if initial numbers of two kinases in different layers are same, in order to distinguish their different signaling abilities, the scaffold binding should be strong enough. Thirdly, the scaffold number can regulate the kinase activation in a large time region. Fourth, it is observed that for slow dephosphorylation case, scaffolds decrease the sharpness of
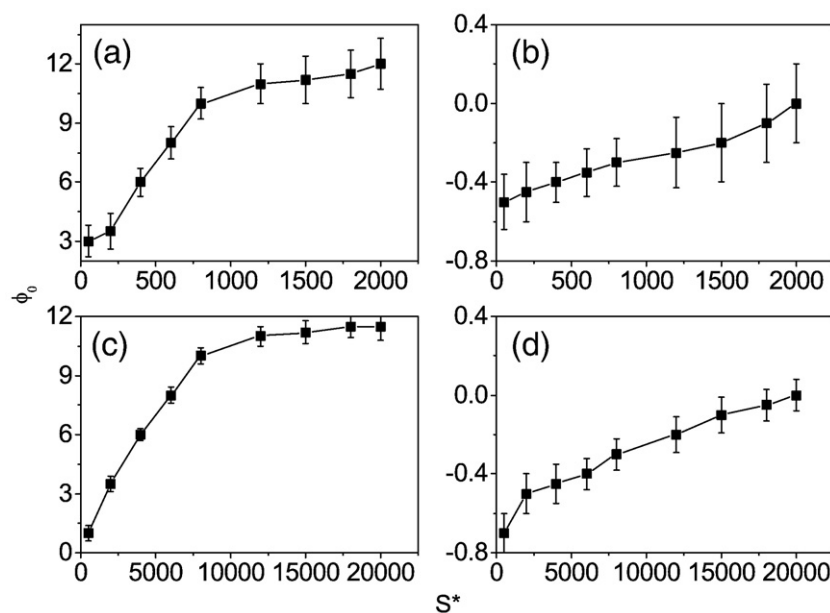

Fig. 11. Dose–response curves for slow dephosphorylation ((a) and (c)) and fast dephosphorylation ((b) and (d)). From top to bottom, the simulation results on a lattice space of 100×100 and $100 \times 100 \times 10$ are shown respectively. The graded response is obvious.
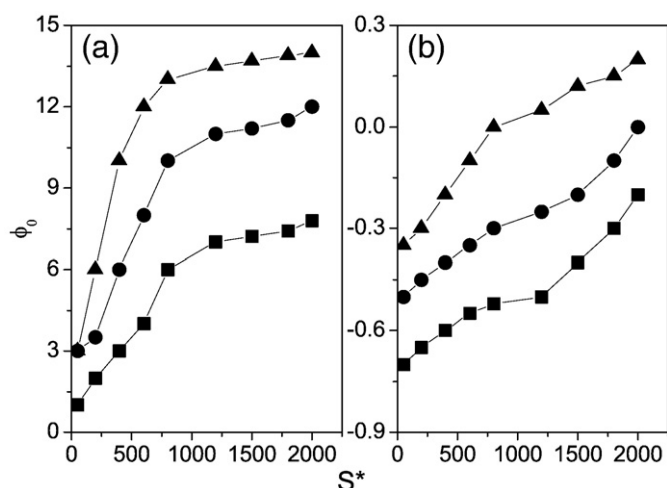
Fig. 12. Dose–response curves for (a) slow dephosphorylation and (b) fast dephosphorylation for different scaffold number, $NS = 0$ (▲), $NS = 200$ (●), and $NS = 800$ (■).

the dose–response curves, while for fast dephosphorylation case, increasing scaffold number decreases the height of response, but the shape of graded response is sustained.

A discussion about signal amplification is given when the input signal S^* is changed. To see its effect, some dose–response curves are plotted in Fig. 11. For simplicity, only $E_{UB} = 7.2$ is considered. (i) On the lattice space of 100×100, scaffold number is 200, the input signal is changed from 200 to 2000. It is observed, for slow dephosphorylation (Fig. 11(a)), the signaling amplification exhibits a graded response, similar to a Michaelis–Menten function. For fast dephosphorylation (Fig. 11(b)), the signaling amplification exhibits a gentle increase. The sensitivity of dose–response under slow dephosphorylation is larger than that under fast dephosphorylation. (ii) System size is an important factor especially in the research of stochasticity in the level of single cell. Some works about the effects of different system size on circadian oscillation and cell cycle are provided by Chemical Langiven Equation and Gillespie method [35,36]. As for the stochastic spatio-temporal model for MAPK cascade we study here, the time scale of diffusion is very small, and it will cost a great deal of simulation time if the system size is very large. Therefore, as an illustration, we provide a further investigation about signaling amplification on a larger size, i.e., the lattice space of $100 \times 100 \times 10$. In order to make this simulation result on system size of $100 \times 100 \times 10$ comparable with that on system size of 100×100, the density of each protein should be unchanged. Therefore, the system we simulated here consists of 2000 A, 2000 B, 10,000 C, and 6000 generic P species. The scaffold number is 2000. It is clear the regulatory property has no qualitative change for two cases, however the increased lattice size is exactly reduced the level of stochasticity entailed in the MC simulations (compared Fig. 11(c) with (a), Fig. 11(d) with (b)). It is noted, a larger lattice space that is closer to real cell size is better in the simulation of cell signaling, however we convince that the qualitative results will remain.

Because scaffolds limit signal amplification when $E_{UB} = 7.2$ (see Fig. 9), we suppose, under these conditions, dose–response curves would appear less sharp in the presence of scaffolds. This is because each stimulating molecule has the ability to activate many more than one downstream target in solution, whereas the scaffold limits this number. Hence, how scaffold proteins control the dose–response is also studied. As shown in Fig. 12, it is observed that for slow dephosphorylation case, scaffolds decrease the sharpness of the dose–response curves and can even convert switch-like response ($NS = 0$) to graded response ($NS = 800$) (see Fig. 12(a)). For fast dephosphorylation case, increasing scaffold number also decreases the height of response, but the shape of graded response is sustained (see Fig. 12(b)).

The novel regulatory roles obtained in our simulation are exactly observed in some specific biological systems. (i) For the constructive role observed in Fig. 5(a), an example is provided by T cells. Dephosphorylation process is slow in T cells [37,38], and the KSR scaffold is known to amplify signaling through the MAPK pathway as measured by ERK activation [39,40]. (ii) For the destructive role observed in Fig. 9, one example is that scaffolding such a cascade using INad inhibits signal amplification in Drosophila [41]. Furthermore, this destructive role of scaffold may explain recent data that demonstrates that mutating the docking site of Fus3 to the scaffold Ste5 results in a larger signal output because it reduces the strength of interaction of this kinase with the scaffold [42]. Of course, a full correlation between our modeling results and real biological systems is difficultly clarified at present. We hope our work may provide some predictions for future experiments.

We only expect to give some qualitative results about the regulatory property of scaffold protein, therefore only two specific cases, i.e., slow dephosphorylation and fast dephosphorylation, are provided. However our simulations are employed in large enough parameter regions for E_{UB} and NS. The flexible regulatory roles of scaffold protein obtained by our modeling show the adaptability of real cascade to the complex cellular environment and physiological state. It should be pointed out that, in order to focus our attentions on the scaffold protein, some biological processes are simplified. For example, we only take one-step sequential phosphorylation process, and still adopt a single-step collision mechanism for the kinase activation or deactivation on the scaffold. To model a real cascade inside a cell, more details should be considered into the combined model. To address these interesting problems, the next work is expected.

Acknowledgments

References

[1] L.F. Chang, M. Karin, Mitogen-activated protein kinases, Nature 410 (2001) 37–40.
[2] M.S. Q., E.A. Elion, MAP kinase pathways, J. Cell Sci. 118 (2005) 3569–3572.
[3] J.W. Locasale, Three-state kinetic mechanism for scaffold-mediated signal transduction, Phys. Rev. E 78 (2008) 051921-1-7.
[4] K.H. Chiam, C.M. Tan, V. Bhargava, G. Rajagopal, Hybrid simulations of stochastic reaction-diffusion processes for modeling intracellular signaling pathways, Phys. Rev. E 74 (2006) 051910-1-13.
[5] H. Qian, T.C. Reluga, Nonequilibrium thermodynamics and nonlinear kinetics in a cellular signaling switch, Phys. Rev. Lett. 94 (2005) 028101-1-4.
[6] S. Tanase-Nicola, P.B. Warren, P.R. ten Wolde, Signal detection, modularity, and the correlation between extrinsic and intrinsic noise in biochemical networks, Phys. Rev. Lett. 97 (2006) 068102-1-4.
[7] F. Tostevin, P.R. ten Wolde, Mutual information between input and output trajectories of biochemical networks, Phys. Rev. Lett. 102 (2009) 218101-1-4.
[8] T. Joneson, D. Bar-Sagi, Ras effectors and their role in mitogenesis and oncogenesis, J. Mol. Med. 75 (1997) 87–93.
[9] C.J. Marshall, Ras effectors, Curr. Opin. Cell. Biol. 8 (1996) 197–204.
[10] M. Marhl, M. Perc, S. Schuster, A minimal model for decoding of time-limited Ca^{2+} oscillations, Biophys. Chem. 120 (2006) 161–167.
[11] M. Marhl, M. Perc, S. Schuster, Selective regulation of cellular processes via protein cascades acting as band-pass filters for time-limited oscillations, FEBS Lett. 579 (2005) 5461–5465.
[12] V. Grubelnik, B. Dugonik, D. Osebik, M. Marhl, Signal amplification in biological and electrical engineering systems: universal role of cascades, Biophys. Chem. 143 (2009) 132–138.
[13] D.K. Pant, A. Ghosh, Automated oncogene detection in complex protein networks with applications to the MAPK signal transduction pathway, Biophys. Chem. 113 (2005) 275–288.
[14] D.K. Pant, A. Ghosh, A systems biology approach for the study of cumulative oncogenes with applications to the MAPK signal transduction pathway, Biophys. Chem. 119 (2006) 49–60.
[15] N. Sengupta, P.K. Vinod, K.V. Venkatesh, Crosstalk between cAMP-PKA and MAP kinase pathways is a key regulatory design necessary to regulate FLO11 expression, Biophys. Chem. 125 (2007) 59–71.

[16] T. Pawson, Dynamic control of signaling by modular adaptor proteins, Curr. Opin. Cell Biol. 19 (2007) 112–116.

[17] K.L. Dodge-Kafka, J. Soughayer, G.C. Pare, J.J. Carlisle Michel, L.K. Langeberg, The protein kinase A anchoring protein mAKAP co-ordinates two integrated cAMP effector pathways, Nature 437 (2005) 574–578.

[18] A. Levchenko, J. Bruck, P.W. Sternberg, Scaffold proteins may biphasically affect the levels of mitogen-activated protein kinase signaling and reduce its threshold, Proc. Natl. Acad. Sci. U. S. A. 97 (2000) 5818–5823.

[19] J.W. Locasale, A.S. Shaw, A.K. Chakraborty, Scaffold proteins confer diverse regulatory properties to protein kinase cascades, Proc. Natl. Acad. Sci. U.S.A. 104 (2007) 13307–13312.

[20] J.W. Locasale, A.K. Chakraborty, Regulation of signal duration and the statistical dynamics of kinase activation by scaffold proteins, PLOS Comput. Biol. 4 (2008) e1000099.

[21] W.R. Burack, A.S. Shaw, Signal transduction: hanging on a scaffold, Curr. Opin. Cell Biol. 12 (2000) 211–216.

[22] R. Heinrich, B.G. Neel, T.A. Rapoport, Mathematical models of protein kinase signal transduction, Mol. Cell 9 (2002) 957–970.

[23] M. Gosaka, M. Marhla, M. Perc, Pacemaker-guided noise-induced spatial periodicity in excitable media, Physica D 238 (2009) 506–515.

[24] M. Gosak, M. Marhl, M. Perc, Spatial coherence resonance in exci biochemical media induced by internal noise, Biophys. Chem. 128 (2007) 210–214.

[25] M. Perc, M. Gosak, M. Marhl, Periodic calcium waves in coupled cells induced by internal noise, Chem. Phys. Lett. 437 (2007) 143–147.

[26] M. Perc, M. Gosak, M. Marhl, From stochasticity to determinism in the collective dynamics of diffusively coupled cells, Chem. Phys. Lett. 421 (2006) 106–110.

[27] M. Gosak, Cellular diversity promotes intercellular Ca^{2+} wave propagation, Biophys. Chem. 139 (2009) 53–56.

[28] Y. Wang, Q.S. Li, System-size resonance for intracellular and intercellular calcium signaling, Biophys. Chem. 136 (2008) 32–37.

[29] H.S. Chen, J.Q. Zhang, J.Q. Liu, Selective effects of external noise on Ca^{2+} signal in mesoscopic scale biochemical cell systems, Biophys. Chem. 125 (2007) 397–402.

[30] K. Takahashi, S.N.V. Arjunan, Space in systems biology of signaling pathways-towards intracellular molecular crowding in silico M. Tomita, FEBS Lett. 579 (2005) 1783–1788.

[31] M. Dobrzynski, J.V. Rodriguez, J.A. Kaandorp, J.G. Blom, Computational methods for diffusion-influenced biochemical reactions, Bioinformatics 23 (2007) 1969–1977.

[32] B.N. Kholodenko, Cell signalling dynamics in time and space, Nat. Rev. Mol. Cell Biol. 7 (2006) 165–176.

[33] H. Berry, Monte Carlo simulations of enzyme reactions in two dimensions: fractal kinetics and spatial segregation, Biophys. J. 83 (2002) 1891–1908.

[34] D.A. Lauffenburger, J.A. Linderman, Receptors: Models for Binding, Trafficking, and Signaling, Oxford University Press, 1993.

[35] M. Yi, Y. Jia, Q. Liu, J. Li, Enhancement of internal noise coherence resonance by modulation of external noise in a circadian oscillator, Phys. Rev. E 73 (2006) 041923-1-8.

[36] M. Yi, Y. Jia, J. Tang, X. Zhan, L. Yang, Q. Liu, Theoretical study of mesoscopic stochastic mechanism and effects of finite size on cell cycle of fission yeas, Physica A 387 (2007) 323–334.

[37] A. von Kriegsheim, A. Pitt, G.J. Grindlay, W. Kolch, A.S. Dhillon, Regulation of the Raf-MEK-ERK pathway by protein phosphatase 5, Nat. Cell Biol. 8 (2006) 1011–1102.

[38] M.K. Dougherty, J. Muller, D.A. Ritt, M. Zhou, X.Z. Zhou, T.D. Copeland, T.P. Conrads, T.D. Veenstra, K.P. Lu, D.K. Morrison, Regulation of Raf-1 by direct feedback phosphorylation, Mol. Cell 17 (2005) 215–224.

[39] D.A. Ritt, I.O. Daar, D.K. Morrison, in: W.E. Balch, C.J. Der, A. Hall (Eds.), Regulators and Effectors of Small GTPases: Ras Family, vol. 407, Academic, New York, 2006, pp. 224–237.

[40] A. Nguyen, W.R. Burack, J.L. Stock, R. Kortum, O.V. Chaika, M. Afkarian, W.J. Muller, K.M. Murphy, D.K. Morrison, et al., Kinase suppressor of Ras (KSR) is a scaffold which facilitates mitogen-activated protein kinase activation in vivo, Mol. Cell. Biol. 22 (2002) 3035–3045.

[41] K. Scott, C.S. Zuker, Assembly of the drosophila phototransduction cascade into a signaling complex shapes elementary responses, Nature 395 (1998) 805–808.

[42] R.P. Bhattacharyya, R. Remenyi, M.C. Good, C.J. Bashor, A.M. Falick, W.A. Lim, The Ste5 scaffold allosterically modulates signaling output of the yeast mating pathway, Science 311 (2006) 822–826.